

A Consolidated Multi-State Orbit Estimation Paradigm for Improved RSO Track Custody

Emily Gerber, Thomas Kelecyc, Bill Delude and Bill McClintock

The Stratagem Group Inc, Aurora, CO

ABSTRACT

One of the key enablers for maintaining custody of active Resident Space Objects (RSOs) is persistent coverage which is realized by using tracking observations from geographically dispersed sensors. Adequate coverage that limits surveillance gaps ensures that any RSO maneuver can be detected and tracked in a timely fashion, though this alone is not sufficient criteria for maintaining custody. Coordination of multiple sensor systems must ensure consistent and calibrated tracking data since biased or inconsistent measurements will limit overall tracking quality. A process was developed to provide consistent data quality assessment for an operational constellation of space-based Electro-Optical (EO) sensors. Using a multi-state Unscented Schmidt Kalman Filter (USKF), the process leverages consolidated measurement and state information to provide a more robust and timely data quality assessment. This processing paradigm also provides the metrics needed to classify space-based observation anomalies. In this work the USKF pre- and post-fit measurement residuals and McReynold's filter-smoother consistency test are leveraged to distinguish between sensor data anomalies, RSO maneuvers and space-based sensor platform positional errors.

The goal of this work is to demonstrate improved custody performance in the presence of both data anomalies, RSO maneuvers and sensor positional state errors using representative observation cadences for a space-based constellation of EO sensors which are processed using the multi-state USKF. Representative observations include appropriate applications of lighting and detection constraints, tracking cadences, and revisit times that are derived from operational systems. The space-based sensors include both Geosynchronous Earth Orbit (GEO) and Low Earth Orbit (LEO) systems tracking GEO objects. Different RSO maneuver types and magnitudes are modelled and evaluated for custody maintenance as a part of this study. Detection and estimation of sensor state errors are also examined. The results demonstrate the ability to autonomously and reliably distinguish between sensor data anomalies, RSO maneuvers and sensor positional state errors while maintaining custody of the maneuvering RSO. This implementation lends itself to a reliable autonomous assessment of data quality anomalies and RSO custody in the presence of maneuvers.

Keywords: Unscented Schmidt Kalman Filter (USKF); Track custody; Data anomaly; Track anomaly.

1. BACKGROUND AND MOTIVATION

In 2021, there were 1,807 objects launched into orbit, which was an increase of 41.8% of objects launched in 2020 [1]. The number of objects in space continues to grow year over year, which leads to a need to accurately and efficiently track these objects. Not maintaining custody of RSO's has dangerous consequences, such as a collision and the creation of more orbital debris. Space-based tracking data provides surveillance coverage not encumbered by ground-based sensor

tracking constraints. Additionally, the quality of space-based data is paramount for maintaining safety of flight for all assets.

A multi-state USKF provides a consolidated method to consistently and reliably track objects and provide space domain awareness (SDA) in near real-time. The USKF provides a state estimate of the objects and uncertainty that can be used for SDA quality assessment. What if the filter is producing unexpected results? A filter is susceptible to a lot of internal and external factors. For example, if the RSO maneuvers or lacks observability due to the sensor/RSO geometry, the filter can diverge and provide unusable results and loss of custody of the object. If the data being processed in the filter has an unknown bias, unknown reference frame, or other outliers, these unknowns result in unusable data. In the filter, if the object propagation model insufficiently represents orbital perturbations, is poorly tuned or contains large data gaps, the large resulting covariances will impact filter performance. With a plethora of reasons that a filter could have undesirable outputs, there is a need for autonomously identifying the root cause of the issue. Identifying and addressing these issues provides the best solution for maintaining track custody of objects and ensuring the quality of the filter data for SDA purposes.

Different filter issues have unique signatures, and if appropriately classified (e.g., using Machine Learning) can lead to the autonomous identification and resolution of the root cause. An object maneuvering produces “tells” in the filter output, like a poker player fidgeting with his/her chips before going all in on a bluff. Additionally, sensor and sensor platform issues create their own unique signatures/tells that can be identified. Characterizing these tells in the filter output allow for the determination of the root cause of issues in the filter. By examining filter metrics produced by multiple RSOs being tracked by multiple sensors, the multi-state filter enables isolation of sensor anomalies or RSO specific deviations from the expectation, such as maneuvers.

The USKF output and a series of different tests and metrics, such as the pre- and post-fit measurement residuals and McReynold’s consistency test, give insight into when the filter encounters a maneuver or data anomaly. With interesting results for a single RSO/Sensor, it can be difficult to determine if the issue is from the RSO or the sensor. The multi-state USKF implementation allows for multiple RSO’s with data from multiple sensors to be processed in the same filter at the same time. The following implementation allows for the anomaly to be characterized as an RSO maneuver or sensor data quality anomaly.

- If the artifacts of the issue appear across multiple sensors for a single RSO, then it is an indication of an RSO maneuver. If a maneuver is identified, then the process noise and covariance can be automatically increased to attempt to track the RSO through the maneuver and maintain custody.
- If the artifacts appear across multiple RSOs and a single sensor, then it is an indication of a sensor data anomaly. If a sensor data quality anomaly is detected, then the sensor can be removed from processing to avoid processing anomalous data and producing inaccurate results that could be disseminated to other SDA users. The sensor anomaly can then be evaluated offline, and the sensor can be considered again for processing after the anomaly has been resolved. This process helps to ensure only the highest quality SDA data is produced.

This paper demonstrates use of the multi-state USKF implementation and how it is applied to distinguish between RSO maneuvers and sensor data quality anomalies. The different tests and metrics are outlined and the methodology for determining the type of anomaly is discussed. The process for simulating the RSO maneuvers, sensor biases, and sensor platform errors is provided. The paper focuses on the specific characteristics that are produced by the different anomalies and how they are used to determine the type of anomaly. Results show how an anomaly is detected and the improved track custody with anomalous data removed. The paper concludes with a summary of the results and recommendations for future work and improvements to the process.

2. USKF IMPLEMENTATION FOR MANEUVER AND ANOMALY DETECTION

This section outlines the multi-state USKF implementation and the different tests and metrics that are used for the maneuver and anomaly detection. The USKF was chosen for its ability to model non-linear dynamics through sigma-points, use Ignore, Consider, and Estimate (ICE) parameters for estimating the timing bias, and use a multi-state implementation.

Unscented Schmidt Kalman Filter Implementation

The orbit determination and prediction process are an integral piece of identifying maneuvers and data quality anomalies. It assumes *a priori* knowledge of the data (measurement) errors and their statistics, as well as the dynamic models being used for the estimation and prediction. Proper tuning of the initial state covariances and process noise are essential to producing trusted results. Details of the USKF implementation can be seen in Figure 1 [1].

$$\begin{array}{c}
 \hline
 \text{USKF} \\
 \hline
 \text{Predictive} \\
 S_{zz,k-1} = \text{Cholesky}(P_{zz,k-1}) \\
 Z_{i,k-1} = \hat{z}_{k-1} \pm \sqrt{n_x + n_c} s_{i,k-1} \\
 \text{where } S_{zz} = [s_1, \dots, s_{n_x+n_c}] \\
 w = \frac{1}{2(n_x+n_c)} \\
 Z_{i,k} \leftarrow \dot{Z}_i = f(Z_{i,k-1}, t) \\
 \hat{z}_k = \sum_{i=1}^{2(n_x+n_c)} w_i Z_{i,k} \\
 P_{zz,k} = \sum_{i=1}^{2(n_x+n_c)} w_i (Z_{i,k} - \hat{z}_k)(Z_{i,k} - \hat{z}_k)^T \\
 \hline
 \end{array}$$

Figure 1: USKF algorithm [1]

USKF Timing and Range Bias Formulation

A sensor data quality anomaly can come in the form of a sensor timing bias, which can be estimated in the USKF [2]. In order to either estimate or consider the timing bias, it must be included in the USKF state along with any other estimated parameters (e.g. *position, velocity and CrA/m*). The biases are observable in the USKF via the EO measurements. The RSO is tracked by the EO sensor and gives an actual measurement. A predicted measurement is computed using the estimate RSO state and inertial sensor location. The actual and predicted measurements are compared and evaluated for a bias. Any resulting bias is manifested in the residuals. At the time of each measurement update, the state-vector sigma points are used to compute an equivalent set of measurement sigma points, and these are adjusted for the current best estimate of the timing bias as follows:

$$t_{corrected} = t_{observation} - t_{bias} \quad (1)$$

The estimated bias is also applied in the prediction step of the filter. The predicted state is propagated to the measurement time, minus the estimated sensor bias time. This allows for the predicted state and measurement to be computed for the $t_{corrected}$ time. If the timing bias is not estimated in the filter but present in the measurements, then the state update inaccurately places the error into the in-track component of the state. Estimating the timing bias allows the bias to be characterized, and any subsequent deviations to bias to be detected. The deviation in the characterize bias is used for determining if there is a sensor data quality anomaly.

Multi-state USKF Implementation

The state used in the USKF is a combination of the RSO states (position, velocity, and area to mass ratio) and the sensor timing bias estimates. There can be any combination of RSOs and sensors included in the filter state. The filter state shown here contains N RSOs and M sensors. The total state is defined as follows:

$$\vec{X} = \begin{bmatrix} \vec{X}_{RSO,1} \\ \vec{X}_{RSO,N} \\ \delta\vec{t} \end{bmatrix} \quad (2)$$

The RSO states (1 to N) contain the position, velocity, and area to mass ratio estimates:

$$\vec{X}_{RSO,N} = \begin{bmatrix} \vec{r}_{RSO,N} \\ \vec{v}_{RSO,N} \\ \gamma_{RSO,N} \end{bmatrix} \quad \text{where} \quad \vec{r} = \begin{bmatrix} r_x \\ r_y \\ r_z \end{bmatrix}, \quad \vec{v} = \begin{bmatrix} v_x \\ v_y \\ v_z \end{bmatrix}, \quad \text{and} \quad \gamma = C_r \frac{A}{m} \quad (3)$$

Where C_r is the SRP coefficient, A is the effective cross-sectional area and m is the mass. The sensors (1 to M) include the timing bias estimate:

$$\delta\vec{t} = \begin{bmatrix} \delta t_1 \\ \delta t_M \end{bmatrix} \quad (4)$$

It is important for the bias of a sensor to be characterized to prevent it from biasing the orbit estimates that would be derived from the sensor measurements. Once the bias is known, it can be applied to measurements and deviations in the bias can be detected.

The multi-state implementation is important because if a single sensor and single satellite are processed in the filter, the results are not going to show the data quality anomaly. There is only the single sensor to provide information on the satellite state. If another sensor is added, then that secondary sensor can either confirm the state estimate from the first sensor or it can provide contradiction information. This confirmation/contradiction leads to being able to estimate the errors in the measurements from either sensor.

For a single RSO, the estimated state contains 7 parameters. For the sigma point propagation of a single RSO, the state size increases to 15 (2 times the number of state parameters plus 1). The filter can be generalized for any number of reference satellites, RSOs and tracking sensors, though

the USKF implementation remains as previously described. There is an optimal number of satellites and sensors to be considered in the filter for optimizing the processing time. The simulated scenario for this paper utilizes 10 RSOs and 6 space-based sensors, giving the total size of the filter state being estimated to 76.

Filter Output Metrics

The filter output produces the information needed to determine the quality of the data processed. From within the filter processing, outliers are computed, pre- and post-fit residuals, and the state estimate and covariance are computed. In post processing, the state estimate is compared with the truth state and the filter output is run through a, Unscented Rauch-Tung-Striebel (URTS) Smoother, which is then used to compute the McReynold's consistency metric.

Pre- and Post-fit Residuals

The filter computes a predicted state of the track RSO which gets converted to measurement space. This predicted measurement and covariance is compared with the actual measurement of the RSO from the sensor. This comparison is the pre-fit residual. Then, the filter computes the Kalman Gain and does an update to the filter state and predicted measurement. The same comparison is then made between the "post" updated measurement and the actual measurement. This comparison is the post-fit residual. This calculation shows that the filter update aligned with the actual measurement. The innovation covariance is used to quantify the uncertainty in the residuals. The expected mean and standard deviation of the pre-fit residuals should be on the order of the sensor measurement noise. The post-fit residuals should have a lower mean and standard deviation because of the update from the filter. The pre- and post-fit residuals test evaluates the number of residual data points that fall outside of the innovation covariance. If a percent of the data points that fail exceed a threshold, then the test fails.

State Error Estimate

The estimated state of the RSO is the main output of the orbit determination process. But how do you know if the state estimated by the filter is any good? Using the truth ephemeris that was used to simulate the observations, the truth and estimated states can be compared. This is a good metric to show that the filter has converged and is producing reliable results. It is expected that the estimated state and truth state difference fall within the estimated covariance and converge over time. Unfortunately, in a near-real time scenario, truth ephemeris for RSO's is only available for calibration satellites and often has a high latency. This makes the state error not a useful metric for a near-real time operational system to determine anomalies in an operationally relevant timeline but is useful for validating the results of the filter off-line. The state error estimate test evaluates the number of position and velocity error states that exceed their estimated covariance. If more than a specified percent of data points fails for position and velocity, the entire state estimation error test is determined to have failed.

URTS Smoother and McReynold's Consistency Metric

The output of the filter is used in the URTS Smoother to take account of the information that has been processed. The backwards smoothing allows for a new smoothed state to be computed that leverages information of data that has already been processed. Like the state error metric, this smoothed state can be used as the estimated state to compute the state error. Also from the smoothed results, a consistency metric can be derived. The McReynold's consistency metric is a

measure of the uncertainty in the measurement and the uncertainty in the update. It gives an idea that the update amount falls within the expected range. More information can be found in Figure 2 [3]. An ideal consistency metric is from 0-3, where any value higher than 3 indicates the update does not match the expected uncertainty. This is a very useful metric for determining maneuvers and anomalies within the data. The consistency test evaluates the number of consistency metric points that exceed the 3-sigma threshold. If more than a set percent of consistency metrics fails, the consistency test for that RSO/sensor pair has failed.

McReynolds' consistency check

Define the State and Covariance:	X_k^f = filtered state estimate at time t_k X_k^s = smoother state estimate at time t_k P_k^f = filtered covariance estimate at time t_k P_k^s = smoother covariance estimate at time t_k	
Form the State and Covariance Differences:	$X_{\Delta k} = X_k^f - X_k^s$ $P_{\Delta k} = P_k^f - P_k^s$	<ul style="list-style-type: none"> *If $\text{abs}(R_{\Delta k}^i) \leq 3$ for all i and k, then the test is satisfied globally for each estimate *If $\text{abs}(R_{\Delta k}^i) > 3$ for all i and k, then the filter-smoother test fails globally indicating the possibility of modeling inconsistencies
Define the Consistency Ratio:	$R_k^i = \frac{X_{\Delta k}^i}{\sigma_{\Delta k}^i}$	<ul style="list-style-type: none"> *Thus, position, velocity and A/m estimation performance can be assessed in terms of the ratio of the estimates to the predicted/assumed modeling uncertainties.

Figure 2: McReynold's Consistency Check

Sensor Bias Estimate

There can be multiple sources of sensor biases, but for this work we assume the error is due to an observation timing bias to illustrate the sensor anomaly detection process. The filter estimates a timing bias associated for the sensor and uses the estimated bias to correct the timestamp of measurements processed in the filter. By estimating a bias in the sensors, a source of potential error in the measurements is accounted for and can be sensitive to detecting other data quality anomalies for the sensor, like errors in the sensor state. If the timing bias is not estimated, the error is incorrectly estimated in the in-track component of the state of the RSO. The sensor bias estimate test evaluates if the sensor bias estimate stays within the estimated covariance. If the percent of failed sensor timing bias estimates is above a threshold, then the sensor has a failed test.

3. OBSERVATION SIMULATION AND USE CASES

In order to test the process of determining an RSO maneuver or sensor data anomaly, first RSO maneuvers and sensor data anomalies need to be simulated. The simulation includes an ephemeris generator to propagate the sensor and RSO states for the desired time frame at a specified cadence (lower than the desired tasking cadence). With the generated ephemeris, the states are used to compute EO observations. These observations are constrained by sensor, geometric, and physical constraints. Additionally, the observations are taken at a realistic tasking cadence based on a previous operational study [4]. The simulated measurements are converted into an OPAL (Optical Processing Architecture at Lincoln) Input File (OIF) format. The initial states of the filter are initialized using a two-line element set (TLE) for the tracked RSOs at the time of the initial observations with a default initial covariance representative of expected TLE uncertainties.

The ephemeris generator uses a high-fidelity propagation that propagates the state for 10 GEO RSOs and 6 space-based sensors. The 10 RSOs are geographically dispersed around the GEO belt. The sensors include an equatorial LEO, a polar LEO, and 4 evenly spaced GEO sensors. The

ephemeris starting epoch is May 6, 2022, at 4:00 UTC and the end epoch is May 6, 2022, at 16:00 UTC. The ephemeris is generated at a 5 second cadence. The ephemeris generator incorporates 3-body, sun tides, moon tides, drag, and solar radiation pressure (SRP). The gravity model uses a degree and order of 18. For the sensor platform anomaly of mis-modelled dynamics, the reported state of the observations does not include drag being modelled for the LEO sensors. To model the maneuvers, during the ephemeris generation, after the filter would have converged, the maneuver delta-v is applied to the RSO state at the maneuver time. The new state is then used for propagation of the rest of the ephemeris.

For generating the measurements, first the line of sight is computed. If the RSO is farther than a specified range from the sensor, the RSO is not visible to the sensor. Next, the object is checked for earth, sun, and moon exclusions. Finally, if the visual magnitude is greater than a specified value, then the object is too dim to be detected by the sensor and no observation is created. Access windows of all available visible times are created for all the RSO/Sensor pairs. Then the access windows are used to create a tasking schedule. The tasking schedule includes the tasking cadence of 7 observations per track and a revisit of 10 minutes. A +/- 2 arc-sec Gaussian distribution of noise is applied to all observations. The observations are then converted into a common format that can be read in by the filter.

Analysis Use Cases

Nominal (no maneuvers or sensor anomalies)

The nominal use case uses the 10 RSOs and 6 space-based sensors. There are no maneuvers, biases, or anomalies applied to the data. This use case is used to compare the anomalous data cadences and provide a baseline for expected output and results of the filter tests and metrics.

RSO Maneuvers

A deviation in the expected RSO state can happen for many reasons, intentional (planned maneuver) or unintentional (propellant leak). The deviation or anomaly in the RSO state, for the purposes of this paper, can be assumed due to an RSO maneuver. In-track (along-track) and cross-track maneuvers were applied to 4 of the 10 RSOs that were simulated. 2 m/s, and 3 m/s maneuvers were applied for the in-track and cross-track cases to show how the different magnitudes affect the filter results. The maneuvers are defined in the Radial, In-track, and Cross-track frame, then converted to J2000 inertial frame and applied to the J2000 inertial velocity. Each type of maneuver has a different manifestation in the results of the filter, which are examined more later in the paper. The maneuvers are applied after the filter converges to a steady state. Figure 3 outlines how the maneuvers are applied.

Maneuver Modeling

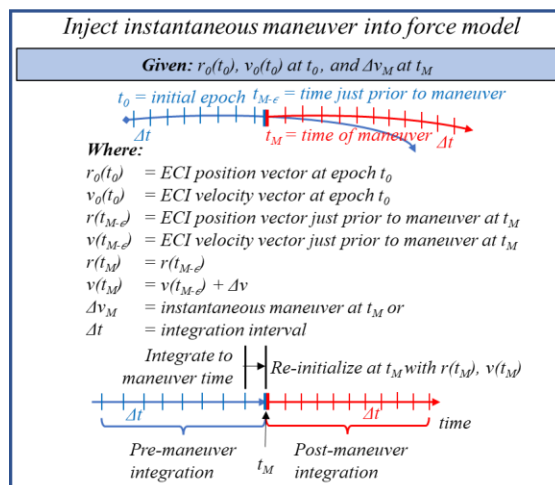


Figure 3: Maneuver Modeling

Sensor Anomalies

To simulate the sensor anomaly, a fixed timing bias is estimated and converged then subsequently falls outside of the calibrated bias. This use case shows that even if the sensor has a well calibrated bias, the process is still able to detect anomalies in the bias. The observations are simulated using the nominal case, but the time-tag that is recorded with the observations has the timing bias applied. The steady-state bias used is 250 milliseconds for a GEO sensor and 300 milliseconds for a LEO sensor. For determining if the bias deviates from the steady state bias an additional 250 millisecond bias is applied to the measurements after the filter converges on the bias. Figure 4 shows the application of the timing bias applied to the measurements.

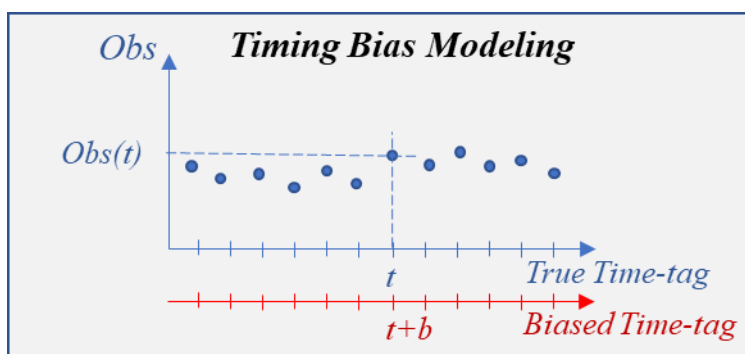


Figure 4: Time Bias Modeling

Sensor Platform Anomalies

The sensor platform anomaly is an error in the satellite state that is carrying the sensor. Mis-modelled dynamics, in the form of drag and SRP, errors are simulated. Similar to the sensor timing bias anomaly, the observations that are recorded are still based on the nominal use case, but the recorded sensor state contains the anomaly. The sensor state needs to be known with high accuracy to provide good filter results. Future work will include estimating the sensor state as a part of the filter. If the sensor platform is using a different dynamics model to determine the state, then this

can cause issues with the downstream SDA products. The mis-modelled dynamics use case uses the nominal observations but records a sensor state that does not include drag modelled for a LEO sensor or a higher CrA/m for a GEO sensor. The filter processing still uses the high-fidelity propagation, including drag for the LEO sensor platform propagation. Figure 5 shows how the sensor platform anomalies are applied to the observations.

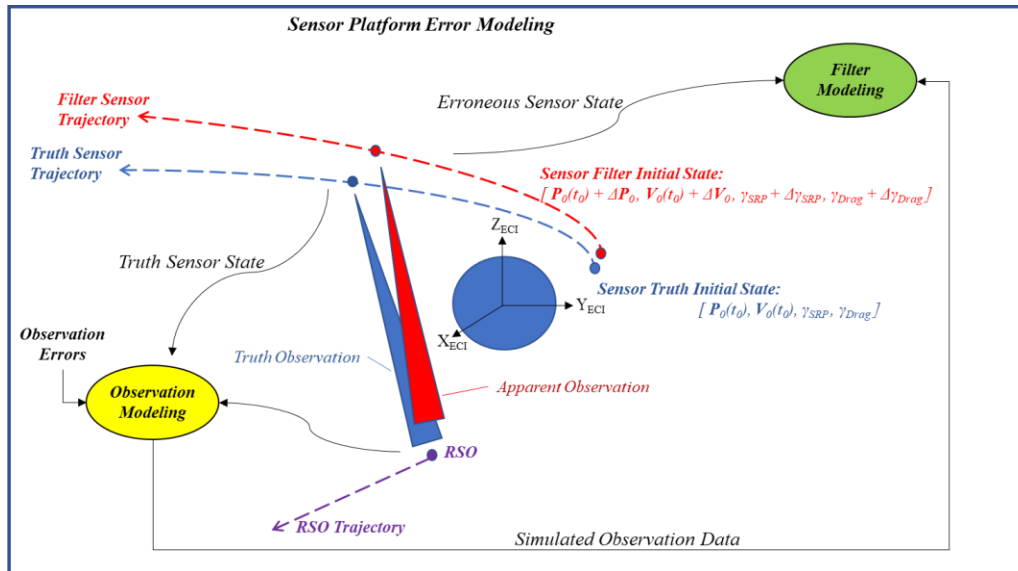


Figure 5: Sensor Platform Error Modeling

4. METRICS FOR MANEUVER AND ANOMALY ASSESSMENT

The goal of the tests and metrics is to determine whether there is an anomaly in the data. Furthermore, the tests and metrics can help to determine the root cause of the anomaly, either from an RSO maneuver or a sensor anomaly. Each individual test used provides a unique insight into the data, but all the tests combined give a more comprehensive understanding of the overall quality of the data. If a combination of tests fails, there is a data quality anomaly present for that sensor and RSO pair, but not enough information to determine if the anomaly was sensor or RSO specific. If there are multiple failed tests for a specific sensor across multiple RSOs, then we can determine it to be a sensor data quality anomaly. Similarly, if there are multiple failed tests for an RSO across multiple sensors, then we can determine the anomaly to likely be an RSO maneuver. Once the determination of anomaly type is made, then the filter can appropriately handle that information to increase track custody and maintain integrity of the data.

RSO Maneuver or Sensor Data Quality Anomaly Determination

The consolidated multi-state-based process uses all the tests to determine if there is an RSO maneuver or data quality anomaly. For each sensor and RSO pair, the tests are run on the simulated data. Each box in Figure 6 represents the total combination status of the different tests for that RSO/Sensor pair. A nominal status, shown in green, represents the sensor and RSO pair data being processed does not have any data quality anomalies being detected. If some of the tests fail, then the status for that sensor and RSO pair is changed to a warning state. If the majority of the tests fail, the status of the sensor and RSO pair becomes an alert for a maneuver or data quality anomaly,

shown in red below. The example graphs of nominal, warning and anomalous states for both and RSO and a sensor can be seen in Figure 6.

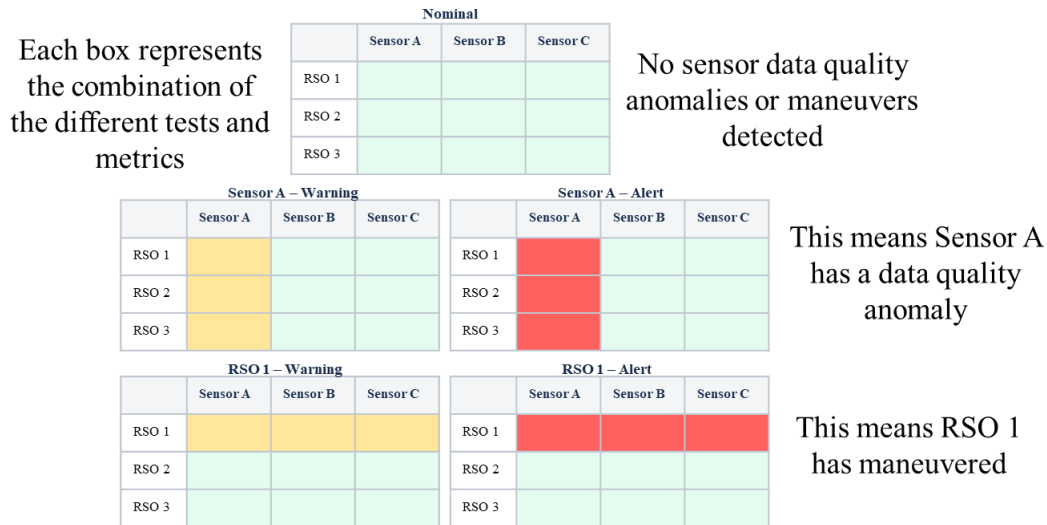


Figure 6: Consolidated Multi-state-based Anomaly Detection Process

The process then determines if the combination of failed tests is due to the result of either a sensor or RSO data quality anomaly. If the failed tests are consistent across a specific satellite or sensor, that that determines whether the data quality anomalies belong to a sensor or RSO.

If there is an RSO maneuver detected, the covariance of the RSO state is increased to attempt to reconverge on the true state of the RSO. Additionally, the filter process noise is increased to allow for more uncertainty in the filter updates and trust the measurements more to help with converging on the true state. If there is a sensor data quality anomaly, then the sensor is removed from processing. The data over the time period where the sensor is identified (minus the anomalous data) is re-processed. The processing of the anomalous data in the multi-state filter has artifacts outside of the single sensor, so in order to reset the filter to a nominal state, the data without the anomaly needs to be re-processed. This allows for additional anomalies to be detected and “cleans” the filtered data for detecting anomalies in the future.

5. ANALYSIS AND ASSESSMENT OF ANOMALIES

This section summarizes the analysis results from processing the simulated data use cases. Each case will show the defining characteristics that are used to determine the type of anomaly present.

Nominal – No sensor Anomalies or RSO Maneuvers

In the nominal use case, simulated observations from 10 RSOs and 6 space-based sensors are processed in the USKF. The output tests and metrics are evaluated to determine if there are any maneuvers or anomalies present in the data. For the nominal case, there are no expected maneuvers or anomalies. Some example plots are shown in Figure 7 to demonstrate what the expected results of the filter are. Nominal state error and residual plots show for satellite 27566 (TDRS 10) that the state and velocity errors converge over time and the state estimate stays within the covariance. Additionally, the RA and Dec residuals stay within the innovation covariance and the mean and standard deviation decrease from pre- to post-fit residuals.

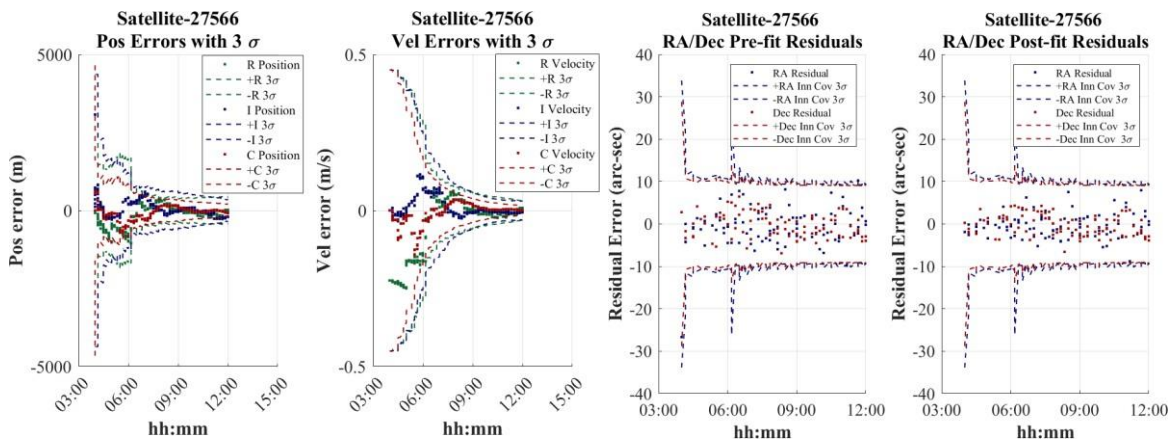


Figure 7: Nominal State Error and Residual Plots

In Figure 8 the nominal Consistency Test shows that all of the sensor bias estimate consistency values stay under the 3-sigma threshold. The consistency metrics for all elements of the position and velocity also are under the 3-sigma threshold. These results are used as the baseline to compare the rest of the anomaly use cases against.

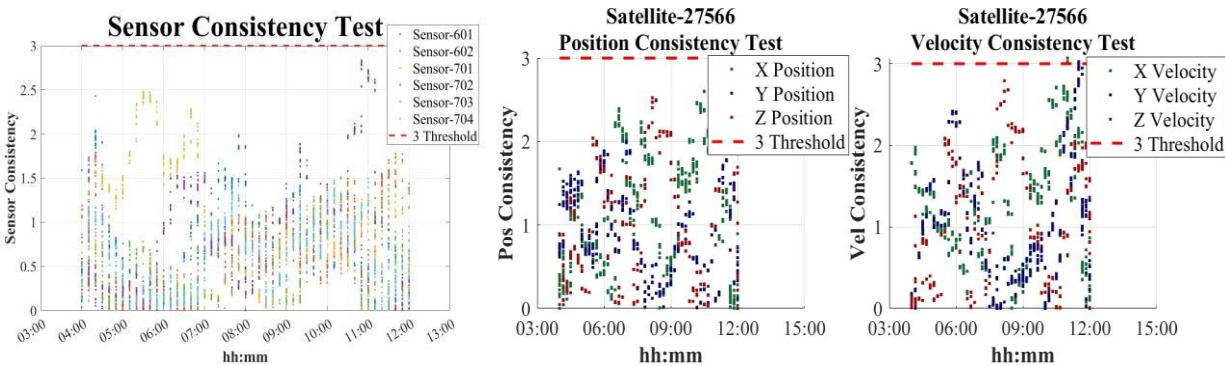


Figure 8: Nominal Consistency Test

RSO Maneuver – In-track and Cross-Track

In the same simulation and filter run, four satellites had maneuvers applied after the filter converged to a steady state. An in-track maneuver was applied to 26313 (TDRS 7) at 2 m/s and 25258 (USA 138) at 3 m/s. A cross-track maneuver was applied to 27566 (TDRS 10) at 2 m/s and to 36411 (GOES 15) at 3 m/s. Only select plots were chosen to demonstrate the unique signatures caused by the in-track and cross-track maneuvers.

In Figure 9 the maneuver state error plots show how the maneuver creates a deviation in the estimated state vs the truth state. The results show that different components of the state are affected by the different types of maneuvers as expected. In this example, the maneuver is intentionally not identified to demonstrate that if the maneuver is not detected, then there is a much higher chance of losing custody of the object.

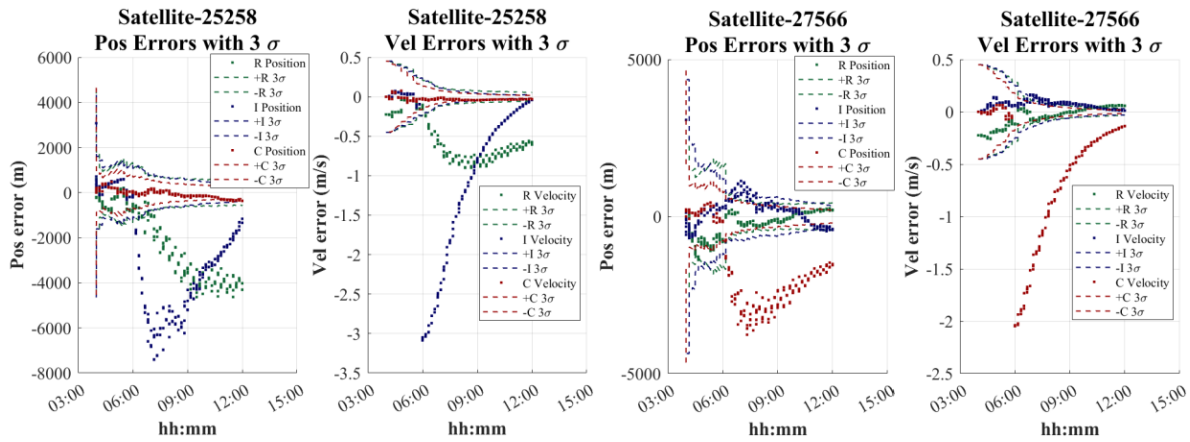


Figure 9: Maneuver State Error Plots

If the maneuver is accurately detected during tracking, then the covariance and process noise can be increased to allow the filter to reconverge on the post-maneuver state. This result gives a much higher chance of being able to maintain custody of the maneuvered object, as shown in Figure 10 maintaining track custody through the maneuver. In addition to the state error, which is not always available, the pre- and post-fit residuals and consistency tests have distinct signatures that can be used to determine a maneuver happened and insight into which type of maneuver.

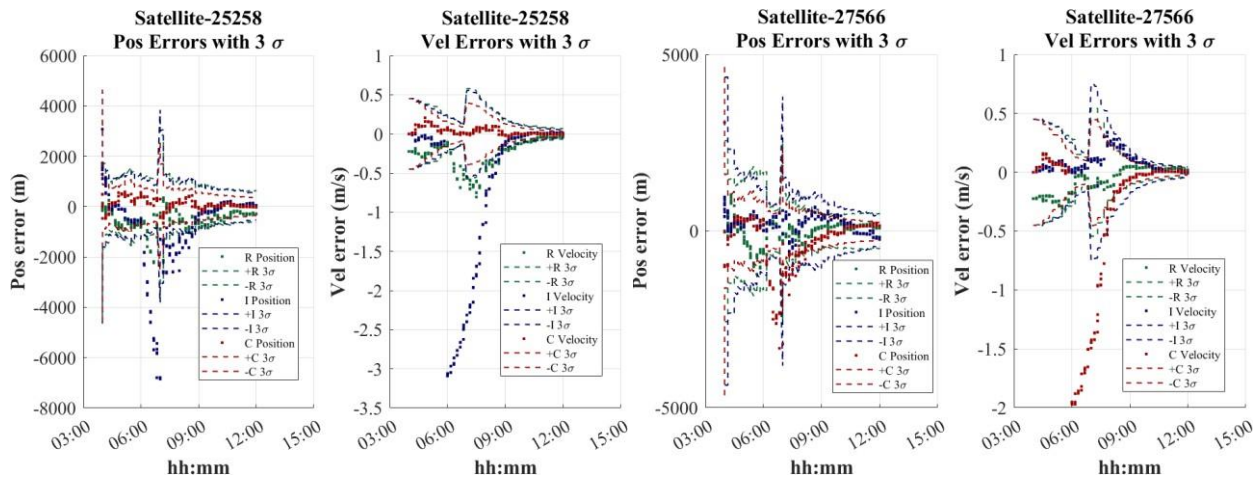


Figure 10: Maintaining Track Custody Through Maneuver

In Figure 11 the maneuver measurement residuals show how the residuals for the satellites fall outside of the innovation covariance. As expected, the Right Ascension is most affected by the in-track maneuver and the Declination is affected by the cross-track maneuver.

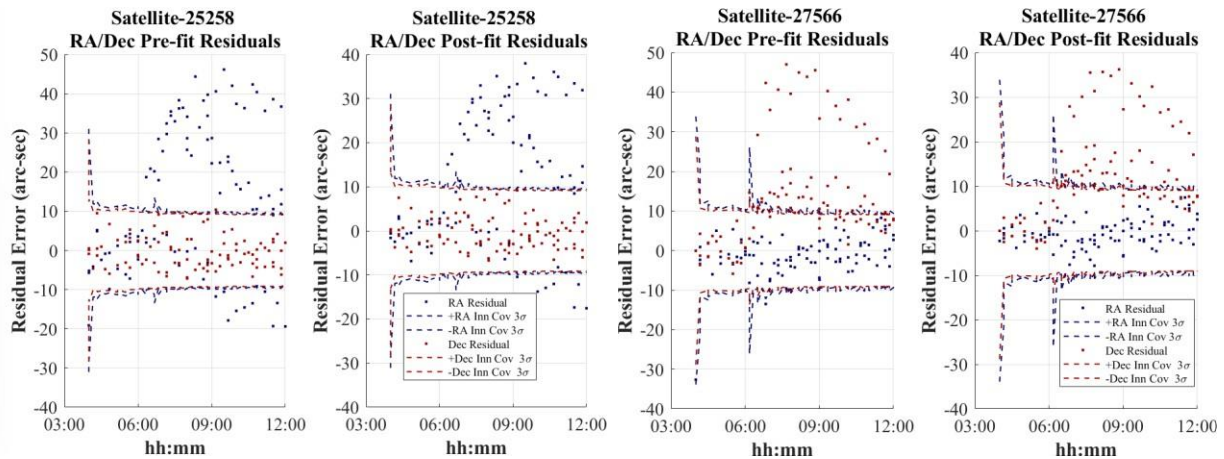


Figure 11: Maneuver Measurement Residuals

Additionally, the consistency test fails in the expected components for the respective maneuvers, as shown in Figure 12 maneuver Consistency Test. With these distinct signatures from the filter output, a maneuver can be determined. The tests fail so that all the tests for a single maneuvered satellite fail across multiple sensors, distinguishing it as a maneuver and not a data quality anomaly. More work needs to be done for evaluating the effectiveness on low-thrust maneuvers and lower-magnitude impulsive maneuvers. Previous work by Kelecy and Jah [5] indicates that the Consistency Test would serve as a good metric for detecting low thrust maneuvers.

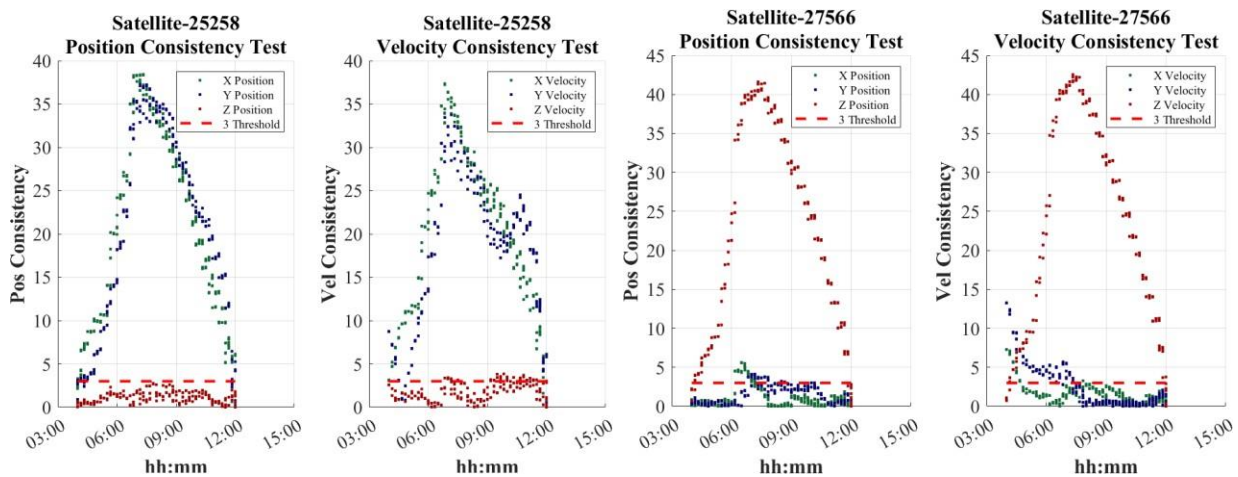


Figure 12: Maneuver Consistency Test

Table 1 shows the full simulation test results. All of the tests for the maneuvering satellites fail, which indicate that the RSOs have maneuvered. There are other failed consistency tests across different sensors (602, 703, and 704) but the other tests for the sensors pass, which show that there is not a data quality anomaly.

Table 1: Maneuver Simulation Results

	601		602		701		702		703		704	
23613	SE	Res										
	CT	BE										

25258	SE CT	Res BE										
27566	SE CT	Res BE										
36411	SE CT	Res BE										
39222	SE CT	Res BE										
40258	SE CT	Res BE										
41838	SE CT	Res BE										
42917	SE CT	Res BE										
43162	SE CT	Res BE										
43917	SE CT	Res BE										

Where SE = State Estimation Error, Res = Pre- and Post-fit Residuals, CT = Consistency Test, and BE = Sensor Bias Estimate.

Sensor Data Anomaly – Timing Bias Deviation

The next use case looks at when a bias is being estimated in the filter, what happens when a deviation occurs for that bias? A 250 millisecond bias is applied to sensor 701 (GEO) and a 300 millisecond bias is applied to 601 (Equatorial LEO). Halfway through the simulation, a deviation in the bias is applied (equal to the original bias applied). The filter is able to notice the deviation occurs and use this to determine there is an anomaly in the data.

Figure 13 shows the timing bias residuals with the bias deviation applied and that all of the residuals stay within the expected values. The mean and standard deviation is higher than expected, but not enough on its own to determine if there is a data quality anomaly.

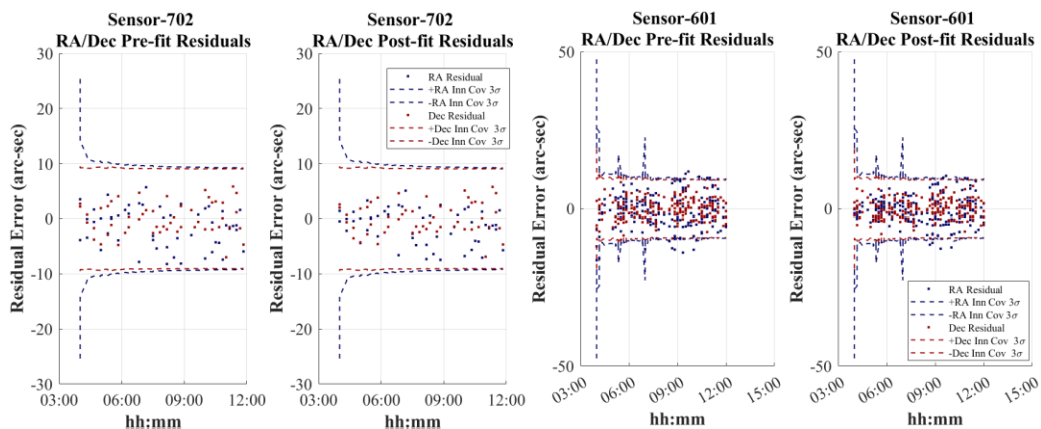


Figure 13: Timing Bias Residuals

Figure 14 illustrates the timing bias estimate where the initial applied bias converges but the deviation in the bias is detected by the filter.

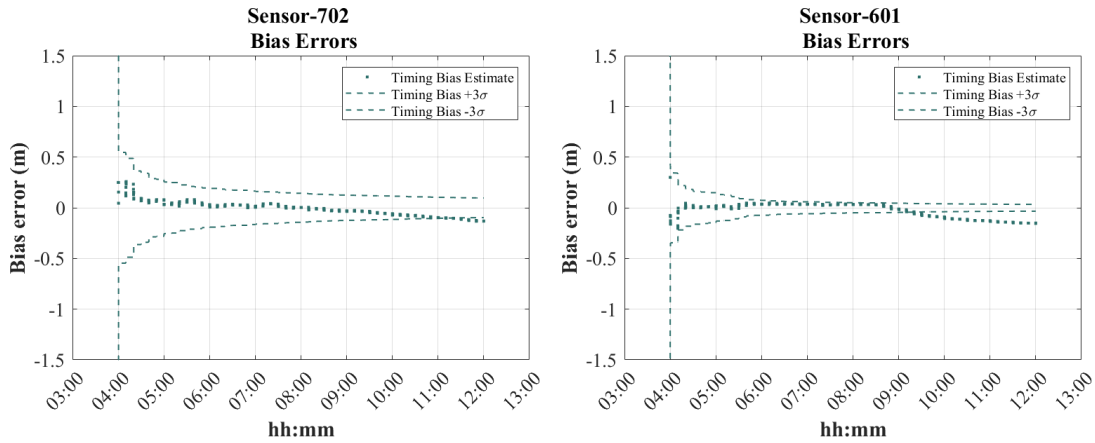


Figure 14: Timing Bias Estimate

Figure 15 shows the timing bias deviation Consistency Test where the consistency test fails for the two sensors with the bias deviation. The combination of tests allows for the determination of a data quality anomaly. The unique signatures point to the timing bias, but more investigation, such as re-estimating a bias and applying it to the data, would be needed to confirm that it is truly a timing bias causing the anomalies in the data.

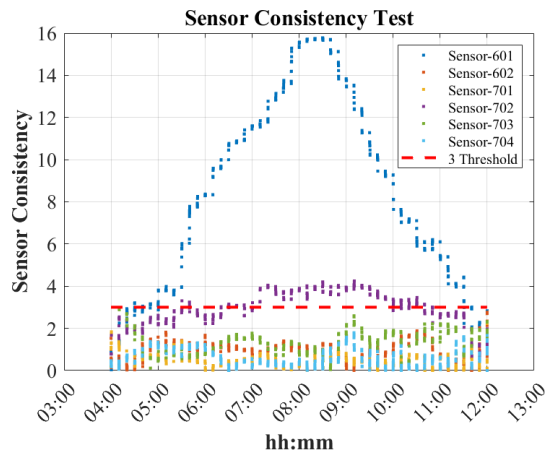


Figure 15: Timing Bias Deviation Consistency Test

Table 2 shows the full simulation results for the bias deviation case. The majority of the tests fail for the two sensors with the bias deviation. Other pre- and post-fit residual tests fail for other satellite sensor pairs, but not enough to detect a data quality anomaly.

Table 2: Bias Deviation Simulation Results

	601		602		701		702		703		704	
23613	SE	Res										
	CT	BE										
25258	SE	Res										

	CT	BE										
27566	SE	Res										
	CT	BE										
36411	SE	Res										
	CT	BE										
39222	SE	Res										
	CT	BE										
40258	SE	Res										
	CT	BE										
41838	SE	Res										
	CT	BE										
42917	SE	Res										
	CT	BE										
43162	SE	Res										
	CT	BE										
43917	SE	Res										
	CT	BE										

Where SE = State Estimation Error, Res = Pre- and Post-fit Residuals, CT = Consistency Test, and BE = Sensor Bias Estimate.

Sensor Platform Position Anomaly – Mis-modelled Dynamics

Another cause of a data quality anomaly comes from different dynamics modelled being used in the filter. In this use case, drag is modelled for creating the observations, but the recorded state of the sensor does not use the same drag model. With the timing bias being estimated in the filter, error from the mis-modelled dynamics gets erroneously estimated as a bias as illustrated in Figure 16 where no sign of an anomaly is apparent.

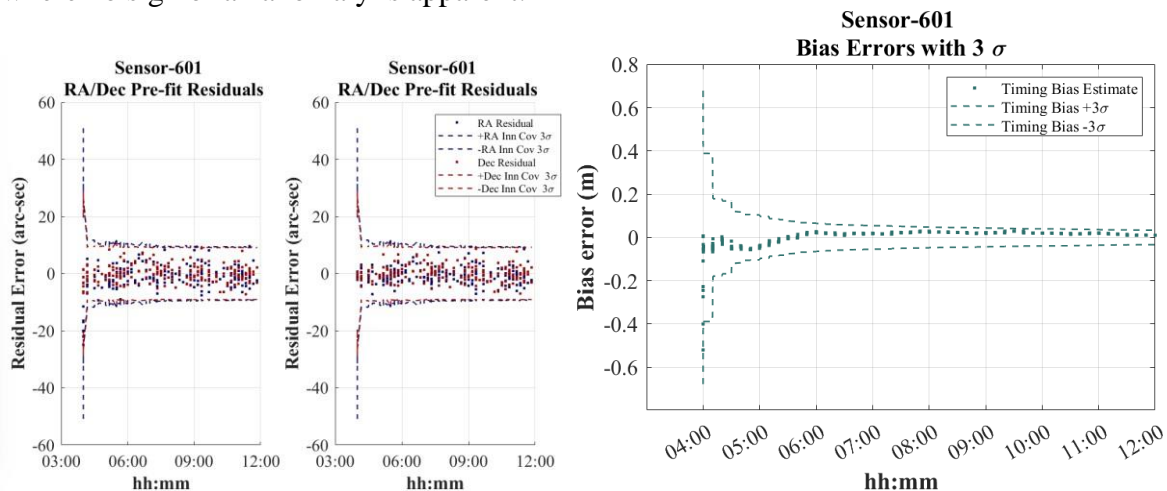


Figure 16: Mis-modelled Dynamics Measurement Residuals and Sensor Timing Bias

This case shows how if there is not a timing bias error, it can be detrimental to estimate a timing bias for the sensors. The filter tries to do an optimization of the fit of the data, which means error can be inadvertently categorized incorrectly. The consistency tests and state estimate tests pass for

all the cases, which would make it difficult to determine the data quality anomaly. Without the timing bias in the filter being estimated, the biggest indicator of a mis-modelled dynamics are the pre- and post-fit residuals for the sensors. In Figure 17 the mis-modelled dynamics measurement residuals (Bias Not Estimated) show the unique signature that can be used to determine that there is a data quality anomaly present for sensor 601 (Equatorial LEO).

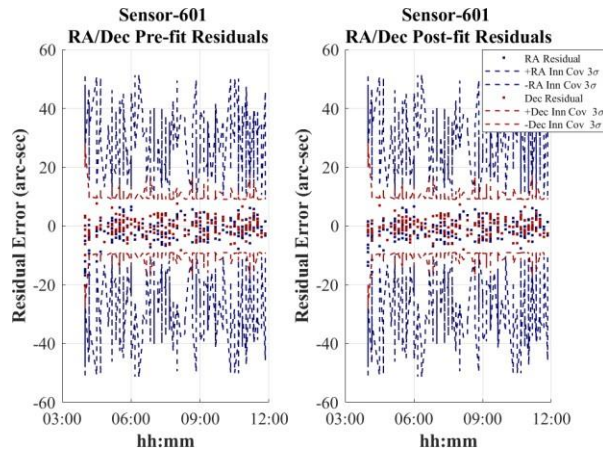


Figure 17: Mis-modelled Dynamics Measurement Residuals (Bias Not Estimated)

Another case of the dynamics being mismodelled would be over-estimating the CrA/m for sensor 704 (GEO). For this case, all of the tests pass except for the consistency test for the timing bias of sensor 704. Figure 18 shows the mis-modelled dynamics Consistency Test with the timing bias being estimated, the consistency test is still able to determine that there is a data quality anomaly for sensor 704.

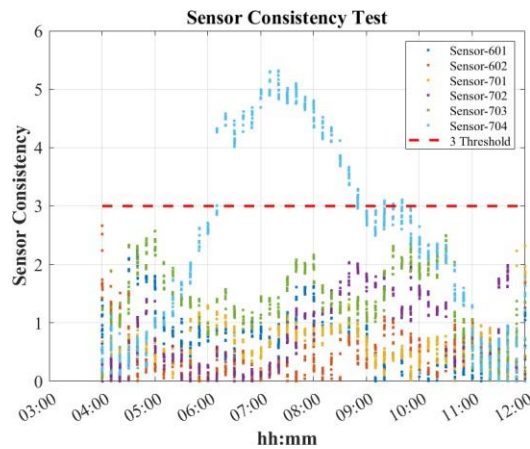


Figure 18: Mis-modelled Dynamics Consistency Test

Table 3 shows the simulation results for the mis-modelled dynamics case where the CrA/m is overestimated in the dynamics model. Not all of the tests for 704 fails, but some do, so it creates a warning state. This can be used to monitor the data coming from 704, but not use it for SDA purposes until the anomaly is resolved.

Table 3: Mis-Modelled Dynamics Simulation Results

	601		602		701		702		703		704	
23613	SE	Res										
	CT	BE										
25258	SE	Res										
	CT	BE										
27566	SE	Res										
	CT	BE										
36411	SE	Res										
	CT	BE										
39222	SE	Res										
	CT	BE										
40258	SE	Res										
	CT	BE										
41838	SE	Res										
	CT	BE										
42917	SE	Res										
	CT	BE										
43162	SE	Res										
	CT	BE										
43917	SE	Res										
	CT	BE										

Where SE = State Estimation Error, Res = Pre- and Post-fit Residuals, CT = Consistency Test, and BE = Sensor Bias Estimate.

6. CONCLUSIONS AND FUTURE WORK

The multi-state USKF filter results and metrics have been applied to several anomaly use cases to demonstrate its ability to distinguish between RSO maneuvers and sensor data quality anomalies and can even provide insight into the type of maneuver and anomaly. The formulation and implementation of the USKF presented and detailed examples utilizing the different output metrics and tests were given. The data simulation process and the maneuver/anomaly determination process were outlined. The results show that for the specific use cases that appropriate application of the filter metrics were able to show the unique signatures caused by maneuvers and data quality anomalies. The maneuver cases show the expected state, residual, and consistency errors in the components from the maneuvers. This result allowed for the maneuver to be detected and the type of maneuver to be surmised. With the ability to use the tests to determine a maneuver has occurred, the filter can react appropriately and open the covariance and process noise to reconverge on the post-maneuver state for maintenance of track custody. The data quality anomaly examples all showed unique signatures that allowed for them to be classified as data quality anomalies; however, more investigation would need to be done to determine the root cause of the anomaly. The estimation of a timing bias can prove beneficial for alerting on deviations in the timing bias

of the sensor but can lead to undesirable results if the anomaly is incorrectly as a timing bias, as shown in the mis-modelled drag case.

Future work will include the simulation of low-thrust maneuvers and analysis on the unique signatures produced. Additionally, representative metrics for each of the use cases can be used in conjunction with Machine Learning techniques to train on the different classes of anomaly and automatically discriminate between the different anomaly types for root cause determination. This process can then be automated to recognize the unique signatures and make the appropriate actions on an operationally relevant timeline.

7. ACKNOWLEDGEMENTS

First off, the primary author would like to thank Thomas Kececy for being a gracious and patient mentor and for his invaluable insight as co-author of this paper. We would also like to thank the Stratagem Group leadership, Brian Bontempo, Ben Aviccoli, Jason Putnam, and Jared Hershman for believing in the value of, and investing in the research presented here. Lastly the authors wish to thank Brian Bontempo and Rad Widman for their review and thoughtful comments.

8. REFERENCES

- [1] J. Stauch and M. Jah, On the Unscented Schmidt-Kalman Filter Algorithm. *Journal of Guidance, Control, and Dynamics* 38(1): 117-123, 2014.
- [2] T. Kececy, E. Lambert, B. Sunderland, J. Stauch, T. Kubancik, V. Mallik, M. Jah, J. Paffett, N. Sánchez-Ortiz and J. Nomen Torres, Automated Near Real-time Validation and Exploitation of Optical Sensor Data for Improved Orbital Safety, IAC-18,A6,10-C1.7,4,x46278, 69th International Astronautical Congress (IAC), Bremen, Germany, 1-5 October, 2018. Copyright ©2018 by the International Astronautical Federation (IAF). All rights reserved.
- [3] Wright, J. R., “McReynolds’ Filter-Smoother Consistency Test,” Internal Analytical Graphics Inc. white paper, May 15, 2009.
- [4] Abernethy, S., E. Gerber. W. Delude, W. Faber, T. Kececy and T. Nave, “Adapting New Processes to Support Improved Space Based Surveillance Ground Operations,” 22nd AMOS Technical Conference, Wailea, Maui, HI, Sept. 14-17, 2021.
- [5] Kececy, T. and M. Jah, “Detection and orbit determination of a satellite executing low thrust maneuvers,” *Acta Astronautica* 66 (2010) 798-809.